

Research Article

Application and extension of diesel spray theory in analysis of methanol spray characteristics under high-pressure injection conditions

Pengbo Dong^a, Yifan Zhang^a, Yang Wang^{a,*}, Wuqiang Long^a, Jiangping Tian^a, Hua Tian^a, Keiya Nishida^{a,b}^a School of Energy and Power Engineering, Dalian University of Technology, Dalian 116024, China^b Graduate School of Advanced Science and Engineering, Hiroshima University, Higashi-Hiroshima 7398527, Japan

A B S T R A C T

Methanol has received widespread attention as a kind of alternative fuel for internal combustion engines because of its wide range of sources, low price, low combustion emission pollution, and carbon neutrality. Meanwhile, the relatively developed diesel spray theories have a great reference value to theoretical analysis of high-pressure methanol injection. Based on the optical experiment of the methanol sprays under high-pressure injection conditions, the empirical models for predicting spray tip penetration, spray angle, spray area, and spray volume of diesel were used to calculate the parameters of the methanol sprays. These calculation values were then compared with the experimental values to establish empirical models of high-pressure methanol spray characteristics. On this basis, an assessment of the adaptability of the diesel spray similarity theory applied to the high-pressure methanol sprays was conducted under similarity conditions. The results show that Wakuri's model has the best predictive performance on the methanol spray tip penetration (the average relative error is 4.31%), and Inagaki's model provides the most precise predictions on the methanol spray angle (the average relative error is 2.63%). After correcting the constants, empirical models that can describe the methanol spray characteristics in this experiment were proposed. In terms of the similarity theory, the diesel spray similarity theory shows good adaptability to the spray tip penetration and spray angle of the high-pressure methanol sprays with nozzle diameters of 0.12 mm and 0.15 mm under similarity conditions. The above results can serve as a basis for extending diesel spray theory to methanol and for the upsizing or downsizing design of direct injection methanol engines with different bore sizes of the same series.

1. Introduction

Internal combustion engines are widely utilized in transportation, energy production, agriculture, military, and other fields because of their high energy density, high thermal efficiency, and fast starting speed. However, massive amounts of pollutants are released by internal combustion engines powered by conventional fossil fuels, aggravating global warming and environmental pollution (Yang et al., 2021; Fayyazbakhsh et al., 2022; Farzaneh et al., 2023; Lloyd et al., 2001; Brijesh et al., 2013; Luo et al., 2024).

In order to slow down this process, a series of regulations have been introduced to reduce emissions (Ravi et al., 2023; Ni et al., 2020; Song et al., 2022). For example, Euro 6 stipulates that diesel vehicles must release no more than 0.08 g of NO_x per kilometer and 0.005 g of particulate matter (PM) per kilometer. The European Union Council even passed a regulation, determining that new cars powered by conventional fuels could not be sold and driven in 2035. As a result, clean energy will become the mainstream fuel for internal combustion engines.

Methanol, as a carbon-neutral fuel, has a wide range of raw material sources, low production difficulties, and ease of transportation. It is

achievable to synthesize methanol from CO, CO₂, and H₂ with solar energy as the energy source, which realizes zero net carbon emissions throughout the whole life cycle (Do et al., 2019; Zhang et al., 2021; Monnerie et al., 2020). As shown in Table 1, compared to traditional fossil fuels, methanol contains lower carbon content and higher oxygen content, which leads to more complete combustion and lower emission levels of soot, CO₂, and NO_x (Garcia et al., 2023; Svensson et al., 2022; Pucilowski et al., 2017; Wu et al., 2024; Su et al., 2020). Due to these advantages, methanol has become a strong candidate for alternative fuels for internal combustion engines in the future.

It has become a consensus that spray characteristics have an important impact on engine performance. Spray characteristics directly affect the distribution of the fuel, evaporation rate, and the degree of atomization, all of which influence air-fuel mixture formation. Finally, it will reflect in emissions and thermal efficiency. The spray characteristics of diesel have been researched profoundly and empirical models have been proposed to describe spray tip penetration, spray angle, and other parameters. Wakuri et al. (1959) developed empirical models of spray tip penetration and spray angle from the perspective of the momentum theory. Hiroyasu and Arai (1990) divided the spray evolution into two

* Corresponding author.

E-mail address: wyclut2010@dlut.edu.cn (Y. Wang).

Table 1
Properties of methanol, diesel and gasoline.

Property	Methanol	Diesel	Gasoline
Chemical model	CH ₃ OH	C ₁₀ –C ₂₂	C ₅ –C ₁₂
Molecular weight	32	220–240	100–115
Density [g/cm ³]	0.7914	0.82–0.88	0.70–0.78
Boiling point [°C]	64.7	175–361	30–200
Autoignition temperature [°C]	470	260	228–471
Lower heating value [MJ/kg]	19.66	42.5	44.5
Latent heat of vaporization [kJ/kg]	1109	270	310
Kinetic viscosity at 20°C [mm ² /s]	0.6	3.7	0.42
Saturated vapor pressure [kPa]	30.997	–	62.0–82.7
Cetane number	3	40–56	0–10
Octane number	112	15–25	80–98

phases bounded by break-up time and summarized the empirical models of break-up length, spray tip penetration, spray angle, and drop size distribution. Naber and Sieber (1996) made some modifications to the analysis of Wakuri. He dimensioned the spray parameters, estimated the constants in the empirical model, and generalized spray tip penetration and time into an inverse relationship. Delacourt et al. (2005) verified Hiroyasu and Arai's models and obtained the models of spray projected area and spray volume by simplifying the spray to a combination of a triangle and a semicircle.

To apply the design information of the existing engines to the engines to be developed, the similarity theory based on empirical models of spray parameters has also attracted widespread attention. Chikahisa and Murayama (1990) theoretically derived the possibility of combustion similarity in diesel engines with appropriate hypotheses and fundamental equations and provided the geometrical similarity conditions. Reitz et al. (2008) established a simple scaling model based on Hiroyasu's empirical model, optimized it with the flame lift-off length, and validated it by numerical simulations. The global engine performance, such as cylinder pressure and heat release rate, could be scaled well based on the scaling law. Inagaki et al. (2016) proved the existence of combustion similarity on two engines under the geometrical similarity condition proposed by Chikahisa with a significant difference in the emission of NO_x and smoke. Therefore, a new spray similarity theory was set up to eliminate the difference after considering flame lift-off length. Zhou et al. (2018, 2020, 2021a, 2021b) theoretically analyzed and experimentally verified the similarity of free sprays and wall-impinging sprays based on three similarity laws. The analysis showed that the wall-impinging spray is difficult to scale accurately. In terms of free sprays, it was found that the pressure rule showed high accuracy in predicting spray tip penetration, spray angle, and excess air ratio, while the speed rule and the lift-off rule led to a smaller spray angle and a larger spray tip penetration. In addition, Zhou et al. also investigated the spray similarity under the three similarity laws with the main-post and pilot-main injection strategies, and the results were similar to the previous studies in that the pressure rule had the best utility, and the other two rules increased the scaled spray tip penetration.

Researchers have also extensively studied the methanol spray characteristics. Gong et al. (2007) studied spray characteristics of medium-pressure direct injection methanol sprays. Under the same experimental condition, spray tip penetration was smaller and the spray angle was larger than diesel. The constants in Hiroyasu's model were modified to describe the spray angle of methanol. Wang et al. (2022) compared diesel and methanol evaporating spray characteristics under high-pressure direct injection conditions. Because of the difference in physicochemical properties, methanol sprays had more irregular boundaries, shorter spray tip penetration, and wider spray angle. When the energy of the injected fuel remained constant, spray tip penetration was rather larger than that of diesel, deteriorating atomization and evaporation of methanol. Matamis et al. (2020) conducted a study of methanol spray on a heavy-duty compression ignition engine and compared it with PRF81 gasoline. The start of injection timing had a

strong impact on the maximum liquid penetration length of methanol. In contrast, ambient density had little effect on methanol, especially compared to PRF18. There was little impact of injection pressure on the maximum liquid penetration length, while mainly affecting the initial growth rate of the spray. Ghosh et al. (2021) researched methanol evaporating spray characteristics with an injection pressure of 200 bar~480 bar. Ambient density significantly influenced both liquid penetration and vapor penetration. When ambient density was approximately doubled, liquid penetration decreased by 30%. While injection pressure had little impact on liquid penetration, it greatly affected vapor penetration. An increase in ambient temperature is observed to reduce liquid penetration, while its impact on vapor penetration is negligible.

As a kind of alternative fuel for internal combustion engines, the research on methanol spray characteristics is not as mature as that of traditional fossil fuels and there are no systematic theories. While methanol is usually applied under conditions similar to diesel engines, to modify the engine to adapt to methanol as well as promote the development of methanol engines, the diesel spray theories serve as a crucial guide. However, due to the properties of methanol, the diesel spray theories usually cannot be directly applied to methanol sprays. The study aims to apply and extend the spray theories of diesel to methanol so that they can accurately describe the methanol spray characteristics.

In this study, the empirical models of spray tip penetration, spray angle, spray area, and spray volume were verified on three injectors with different nozzle diameters. Then, the constants in the empirical models were modified so that they could be used in methanol spray. Finally, the spray characteristics similarity theory derived from Wakuri momentum theory and optimized by Inagaki was employed to prove the existence of methanol spray similarity.

2. Spray theory

2.1. Empirical model

2.1.1. Spray tip penetration

Spray tip penetration is one of the most commonly studied spray characteristics, which can be expressed as an equation involving injection parameters and in-cylinder parameters, such as nozzle structural parameters, injection pressure, in-cylinder temperature, and pressure. Different empirical models have been established for spray tip penetration prediction.

Wakuri et al. (1959) proposed an empirical model of spray tip penetration on the basis of the assumption that "The air in the fuel jet stream forms a kind of mixture with the fuel droplets.", combined with momentum theory.

$$S = C \left(\frac{\Delta P}{\rho_a} \right)^{0.25} \left(\tan \frac{\theta}{2} \right)^{-0.5} d^{0.5} t^{0.5} \quad (1)$$

Where S is spray tip penetration, C is constant, ΔP is the difference between injection pressure and ambient pressure, θ is spray angle, ρ_a is ambient gas density, d is nozzle diameter, and t is time after the start of injection.

Based on the experimental data and jet breakup theory (Levich et al., 1963), Hiroyasu and Arai (1990) derived the following model, dividing the entire injection stage into the before-breakup period and after-breakup period. Spray tip penetration is proportional to time in the first period and to the square root in the second period.

$$S = 0.39 \left(\frac{2\Delta P}{\rho_{fuel}} \right)^{0.5} t \quad (t < t_b) \quad (2)$$

$$S = 2.95 \left(\frac{\Delta P}{\rho_a} \right)^{0.25} (dt)^{0.5} \quad (t \geq t_b) \quad (3)$$

$$t_b = 28.65 \frac{d\rho_{fuel}}{\sqrt{\Delta P\rho_a}} \quad (4)$$

Where ρ_{fuel} is fuel density, and t_b is breaking time.

2.1.2. Spray angle

Spray angle is another commonly studied spray characteristic that directly reflects the spatial distribution of the spray, which is mainly affected by nozzle structural parameters, fuel properties, and ambient gas conditions. Researchers have found that the spray angle will reach a stable value during fuel injection, and most of the empirical models of the spray angle predict this stable value, as a result, they cannot be used for dynamic analysis.

Inagaki et al., 2016 attempted to summarize the spray angles of nozzles with different length-to-diameter ratios in a single expression. Based on experimental data, the empirical model of spray angle was derived through multivariate linear regression analysis."

$$\theta_{\frac{s}{l}} = c \left(\frac{\rho_a}{\mu_a^2} \right)^{0.25} \Delta P^{0.18} \left(\frac{l}{d} \right)^{-0.14} \quad (5)$$

Where μ_a , l refers to ambient gas viscosity, and hole length respectively.

Hiroyasu and Arai (1990) established the following empirical model of spray angle:

$$\theta_{\frac{s}{l}} = 0.0413 \left(\frac{\rho_a \Delta P d^2}{\mu_a^2} \right)^{0.25} \quad (6)$$

Kitaguchi et al. (2012) developed the empirical model of spray angle listed below:

$$\theta_{\frac{s}{l}} = 26 \Delta P^{-0.02} \rho_a^{0.385} d^{0.15} \quad (7)$$

2.1.3. Spray area

Few researchers discussed the change in the spray area. However, it represents the degree of fuel and air mixing, and the size and distribution of the spray area can affect the efficiency of the combustion process. A larger spray area facilitates more effective mixing of fuel and air, which can improve combustion efficiency and reduce the generation of unburned fuel and pollutants.

Equation (8) is an empirical model of spray area:

$$A = \frac{S^2 \tan \frac{\theta}{2} \left(1 + 0.5\pi \tan \frac{\theta}{2} \right)}{\left(1 + \tan \frac{\theta}{2} \right)^2} \quad (8)$$

2.1.4. Spray volume

The study of spray volume is equally significant. When the spray volume is too large, the fuel may turn into larger droplets before entering the combustion chamber, leading to incomplete combustion and low combustion efficiency. On the other hand, when the spray volume is too small, the fuel droplets entering the combustion chamber may become smaller, making it difficult for them to ignite. It can result in increased exhaust emissions and potentially cause diesel engines to lose power.

Delacourt et al. (2005) simplified the entire spray as a triangular surface associated with a semicircular disc and assumed that the cross-section of the spray volume model is similar to the geometry of the spray projected area. Consequently, the empirical model of spray volume can be obtained by integrating the spray area.

$$V = \frac{1}{3} \pi S^3 \frac{\left(\tan \frac{\theta}{2} \right)^2 \left(1 + \tan \frac{\theta}{2} \right)}{\left(1 + \tan \frac{\theta}{2} \right)^3} \quad (9)$$

2.2. Similarity theory

Chikahisa and Murayama (1990) theoretically demonstrated the similarity between diesel engines of different sizes. Combustion can be considered similar if the following conditions are satisfied: 1. Geometrically similar nozzle structure; 2. The nozzle diameter and the hole length are proportional to the bore size; 3. Same swirl ratio; 4. The injection rate is proportional to the product of the ambient density and the cube of the cylinder diameter. 5. Same $N^*D/60u_0$ (where N is engine speed, D is bore size and u_0 is piston speed). According to Inagaki's analysis (Inagaki et al., 2016), the relationship between other parameters can be represented by bore size ratio r , where s refers to a small engine, and l refers to a large engine.

Ratio of bore size:

$$D_s/D_l = r \quad (10)$$

Ratio of nozzle diameter:

$$d_s/d_l = r \quad (11)$$

Ratio of hole number:

$$n_s/n_l = 1 \quad (12)$$

Ratio of hole length:

$$l/d = const \quad (13)$$

Ratio of ambient gas density:

$$\rho_{a,s}/\rho_{a,l} = 1 \quad (14)$$

Ratio of injection pressure:

$$\Delta P_s/\Delta P_l = r^2 \quad (15)$$

In equation (13), the length-to-diameter ratio doesn't change. However, to achieve quantity production, the same series of products typically have the same hole length in practice. Therefore,

$$l/d = 1/r \quad (16)$$

Inagaki determined the relationship between spray characteristics according to the empirical models of spray tip penetration and excess air ratio based on the Wakuri spray momentum theory (as shown in Equations (17) and (18)), as well as the empirical model of spray angle obtained by multiple linear regression analysis (as shown in Equation (19)). Combining the geometrical similarity theory proposed by Chikahisa, the relationship between spray characteristics can be represented by r . The important parameters are shown in the following equation.

$$S \propto \left(\frac{\Delta P}{\rho_a} \right)^{0.25} \left(\tan \frac{\theta}{2} \right)^{-0.5} (d)^{0.5} (t)^{0.5} \quad (17)$$

$$\lambda \propto \tan \theta (\rho_a/\rho_{fuel})^{0.5} (S/d) \quad (18)$$

$$\theta = c (\rho_a \mu_a^2)^{0.25} \Delta P^{0.18} \left(\frac{l}{d} \right)^{-0.14} \quad (19)$$

$$\theta_s/\theta_l = (\rho_{a,s}/\rho_{a,l})^{0.25} (\Delta P_s/\Delta P_l)^{0.18} = (r)^{0.36} \quad (20)$$

$$S_s/S_l = (r)^{0.82} \quad (21)$$

$$\lambda_s/\lambda_l = (r)^{0.18} \quad (22)$$

It is worth noting that the hole length is constant in this study, so equations (20)–(22) should be modified to equations (23), (24), (25).

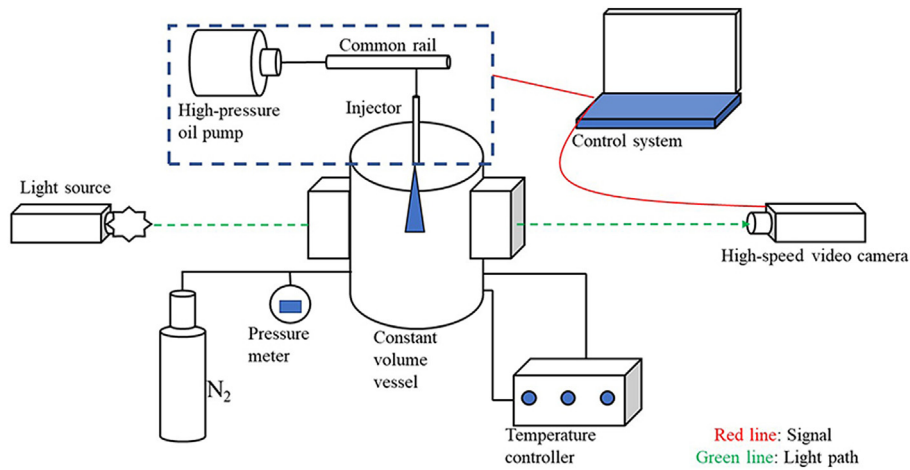


Fig. 1. High-pressure methanol spray optical test system.

$$\theta_s / \theta_l = (r)^{0.5} \tag{23}$$

$$S_s / S_l = (r)^{0.75} \tag{24}$$

$$\frac{\lambda_s}{\lambda_l} = (r)^{0.25} \tag{25}$$

3. Experimental setup and condition

3.1. Experimental setup

The DBI (diffused background illumination) method was used to investigate the spray characteristics of non-evaporating sprays of diesel and methanol. According to the principle of Mie scattering, when the light passes through the observation area, the light intensity is greatly reduced, and the droplets will appear as black parts in the camera. The overall morphology and spray characteristic parameters can be obtained after image processing.

Fig. 1 shows the high-pressure methanol spray optical test system. A constant volume vessel was used to simulate the in-cylinder environment during the operation of an internal combustion engine. It allows to accurately control temperature, pressure, and composition of ambient gas in a wide range. Besides, it is easy to remove the fuel, vapor, and soot on the optical windows. As these advantages are mentioned above, the constant volume combustion bomb is suitable for basic research on spray characteristics. Nitrogen was introduced into the vessel after vacuuming. A temperature controller and a pressure meter regulate the temperature and pressure within the vessel.

To achieve high-pressure injection of methanol and diesel, a high-pressure common rail system with the solenoid injector of Liaoning Xinfeng was employed. In this study, three single-hole injectors with nozzle diameters of 0.12 mm, 0.15 mm, 0.18 mm, and the same hole length of 0.76 mm were used. The nozzle structure is shown in Fig. 2.

The high-speed photography system consisted of a high-brightness light source, and a high-speed camera (FASTCAM SA-Z) with a lens (AF-S VR 70–300 mm f/4.5–5.6G IF-ED). The experiment utilized a resolution of 512 × 896 and a frame rate of 20,000 frames per second. High-brightness light source ensured sufficient background brightness and improved image quality. The visible light from the light source entered the constant volume vessel, passed through the target spray, and was finally captured by the high-speed camera. By adjusting the light intensity and the distance between the light source and the constant volume vessel, the light passing through the spray field became a uniform diffuse background light as much as possible, minimizing the effects of optical path deflection due to gas phase density gradients.

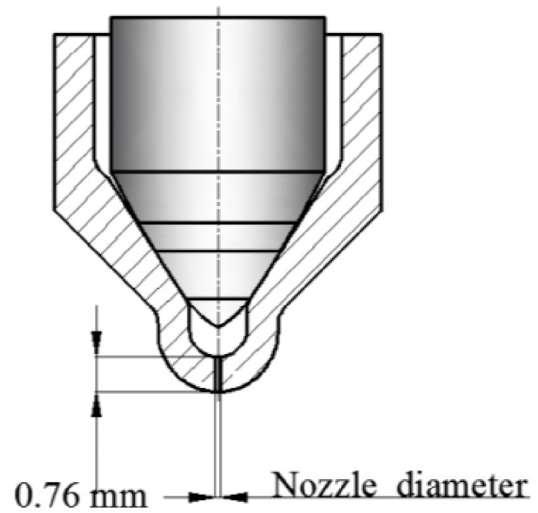


Fig. 2. Scheme of the nozzle configuration.

The high-speed camera shoots in a direction perpendicular to the axis of the sprays. The control system was linked to the high-speed camera and the fuel injection system so that it was able to precisely synchronize fuel injection and photography with NI CompactRIO and LabVIEW.

3.2. Experimental conditions

To verify the empirical formulas and the similarity theory of diesel spray, as well as explore their application in methanol spray, two sets of experimental conditions were set up as shown in Tables 2 and 3.

In the experimental conditions used to verify the empirical formula for spray characteristics, the injection pressure decreases with the increasing nozzle diameters, as shown in Table 2. The nozzle diameters are 0.12 mm, 0.15 mm, and 0.18 mm, corresponding to methanol

Table 2
Experimental conditions.

Item	Methanol			Diesel		
Nozzle diameter [mm]	0.12	0.15	0.18	0.12	0.15	0.18
Injection pressure [MPa]	122	100	47	112	100	40
Ambient temperature [K]	300					
Ambient pressure [MPa]	2					
Ambient density [kg/m ³]	22.45					

Table 3
Experimental Conditions in similarity theory.

Item	Methanol			Diesel		
	0.12	0.15	0.18	0.12	0.15	0.18
Nozzle diameter [mm]	0.12	0.15	0.18	0.12	0.15	0.18
Injection pressure [MPa]	40	70	100	40	70	100
Ambient temperature [K]	300					
Ambient pressure [MPa]	2					
Ambient density [kg/m ³]	22.45					

injection pressures of 122 MPa, 100 MPa, and 47 MPa, and diesel injection pressures of 112 MPa, 100 MPa, and 40 MPa. The ambient temperature is maintained at 300 K to limit the evaporation of methanol and diesel. The ambient pressure was controlled at 2 MPa, and the ambient density was calculated to be 22.45 kg/m³. The experimental conditions in similarity law conform to the similarity theory (equations (11)–(16)), with the injection pressure increasing with the nozzle diameter, as shown in Table 3. The nozzle diameters are 0.12 mm, 0.15 mm, and 0.18 mm, corresponding to methanol and diesel injection pressures of 45 MPa, 70 MPa, and 100 MPa. The ambient temperature, pressure, and density are the same as those in Table 2.

To minimize experimental error, five repetitive tests were performed under each working condition. The spray characteristic parameters in the following sections were averaged from the five tests. It should be noted that, because of the solenoid injector used in this experiment, there was a phenomenon that the injection delay varied with the injection pressure. For easy comparison, the starting point of injection was determined by the spray images.

The spray characteristics studied in this paper include spray tip penetration, spray angle, spray area, and spray volume. Before the discussion, it is necessary to define them separately. The definitions of spray characteristics parameters are shown in Figs. 3 and 4. Spray tip penetration is defined as the vertical distance between the spray tip and the nozzle tip along the axis of the injector. Spray angle is defined as the angle at half of the spray tip penetration. Spray area is defined as the area surrounded by the spray boundary. Based on the spray image, the spray boundary is obtained. The volume V_i for integration can be achieved by rotating the stripe around the axis of each slice of the target spray, where

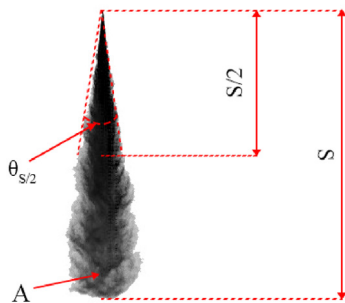


Fig. 3. Definition of spray tip penetration, spray angle, and spray area.

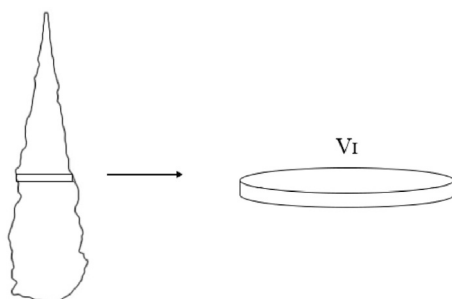


Fig. 4. Definition of spray volume.

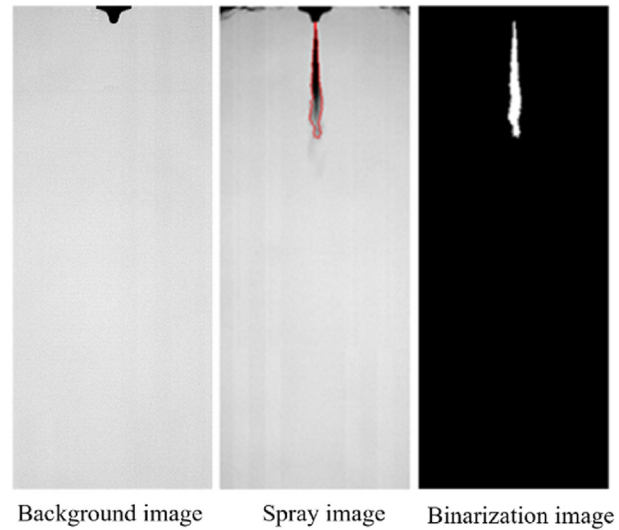


Fig. 5. Schematic diagram of image processing.

i is the number of the pixels over the length, and the sum of the volume of the slices within the spray tip penetration is the total volume of the spray.

3.3. Image processing method

Fig. 5 shows the schematic diagram of image processing. As shown in Fig. 5, the spray image captured by the DBI method has an obvious boundary compared to the background. The spray image was subtracted from the background image by the self-written MATLAB program. After adjusting the threshold to a suitable value, the spray boundary could be obtained, which is marked as the red line. Then the spray image with the red line was binarized and the background was removed to obtain the spray characteristic parameters.

4. Result and discussion

4.1. Empirical model

4.1.1. Spray profiles

Fig. 6 shows the spray profiles of methanol and diesel under experimental conditions listed in Table 2. It can be observed that the development of methanol and diesel sprays is similar. However, the overall spray shape of diesel is narrower and longer than methanol. The shape of the spray head of methanol is more irregular with more folds, indicating that methanol is more prone to air entrainment and facilitates fuel atomization. In the case of 0.12 mm-122 MPa, the initial development of the methanol spray shape is closer to a fan shape in the initial stage. As the injection continues, the differences in spray shape between methanol and diesel decrease and become almost identical at 1.0 ms after the start of injection (ASOI). It can be observed that the non-evaporating sprays of methanol and diesel have similar shapes, which illustrates the possibility of applying diesel spray theories to methanol sprays.

4.1.2. Spray tip penetration

Fig. 7 compares the experimental and calculated values of spray tip penetration of diesel and methanol under the experimental conditions in Table 2. In this study, Wakuri's model and Hiroyasu's model were used for prediction. Wakuri's model inputs the spray angle, and the constant C is obtained from experimental data using the least squares method ($C = 1.274$ for diesel conditions and $C = 1.264$ for methanol conditions). According to Hiroyasu's model, all test points were after breakup time, so only the second part of Hiroyasu's model was used in this study.

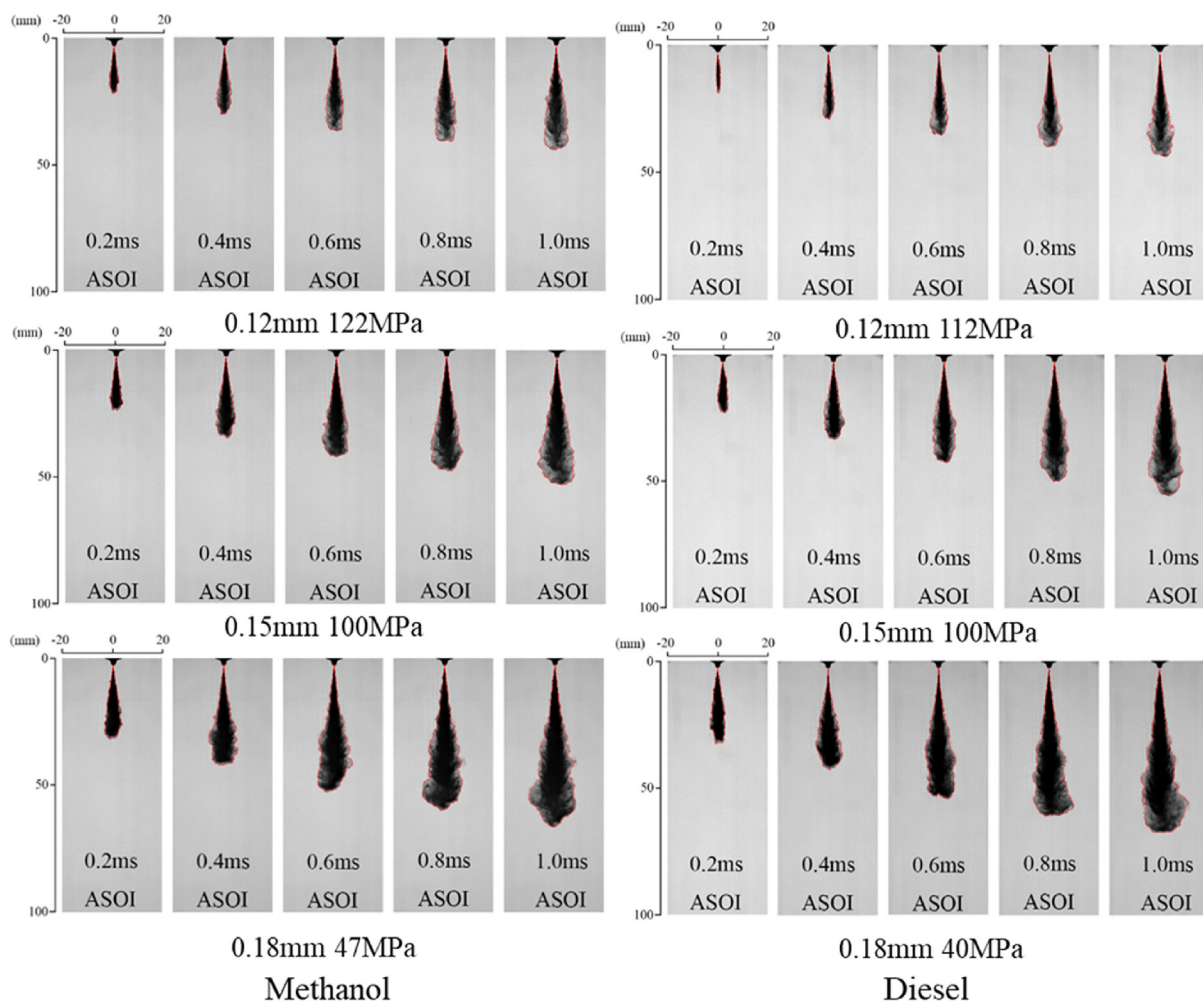
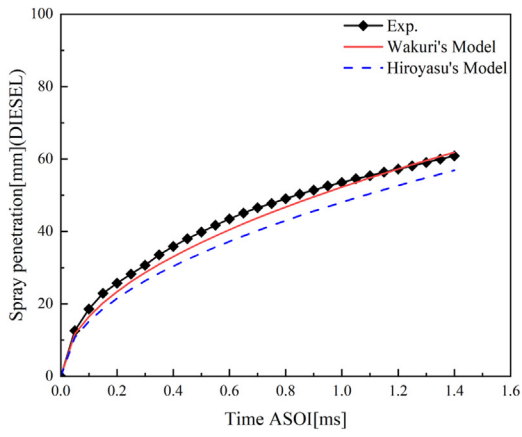


Fig. 6. Spray profiles.

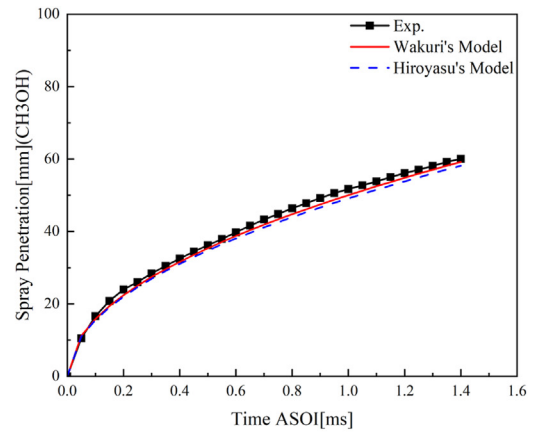
Under diesel conditions, Wakuri's model has the best prediction performance, while Hiroyasu's model underestimates the predicted values and gradually deviates from the experimental values. That's because Hiroyasu's model is based on low injection pressure conditions (7.0~15 MPa), which differs from the high-pressure injection conditions in this study. Furthermore, in Wakuri's model, the use of experimentally measured spray angle as input may also affect the predictive ability of the model, resulting in higher prediction accuracy of Wakuri's model compared to Hiroyasu's model. It is worth noting that under methanol conditions, both of the models have high prediction accuracy, where the average relative error of Wakuri's model is 4.31% under 0.12 mm-122 MPa. According to Table 1, methanol has a lower density and viscosity than diesel. The lower density of methanol results in a lower mass of injected methanol at the same time, and the initial kinetic energy of the droplets is also lower. The lower viscosity and inertia during interaction with the ambient gas make the droplets easier to break up and be influenced by the resistance of the ambient gas, inhibiting the movement of the droplets in the axial direction. Therefore, the spray tip penetration of methanol is smaller than that of diesel, which is consistent with previous results (Wang et al., 2022; Gong et al., 2007). It coincides with the smaller predicted value of Hiroyasu's model, so it shows better prediction results than diesel. From the results, it is clear that the spray tip penetration of diesel and methanol are not significantly different, so the empirical model of diesel can be applied to predict methanol spray tip penetration with high accuracy.

4.1.3. Spray angle

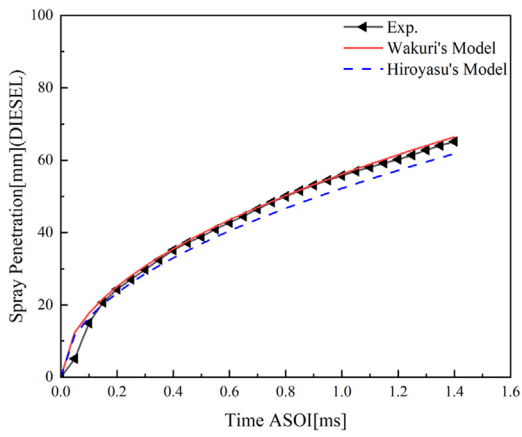
Fig. 8 shows the variation of experimental and calculated values of the spray angle of diesel and methanol under experimental conditions in Table 2 over time. In this study, Inagaki's model, Hiroyasu's model, and Kitaguchi's model were used. The constant C in Inagaki's model was determined based on experimental data with the least-square method ($C = 0.00152$ for diesel conditions and $C = 0.00176$ for methanol conditions). Fig. 8 indicates that Inagaki's model has the highest accuracy under diesel conditions, while Hiroyasu's model overestimates and the Kitaguchi's model underestimates the results with slightly higher accuracy than the former but there is still a large gap between the predicted and the experimental values. Nozzle diameter, hole length, and other nozzle structure parameters will affect the spray angle, and the nozzle used to derive the empirical model differs from the nozzle used in this study, leading to considerable discrepancies between predicted and experimental values. The prediction accuracy of the three models under methanol conditions is not significantly different from those under diesel conditions. Inagaki's model still exhibits the highest accuracy (average relative error of 2.63%), but the matching degree of the predicted and experimental spray angles is lower than diesel. Due to the differences in properties between methanol and diesel, the axial momentum of methanol droplets is suppressed and converted into radial momentum, resulting in a wider spray angle and a marked difference between the predicted and experimental values.



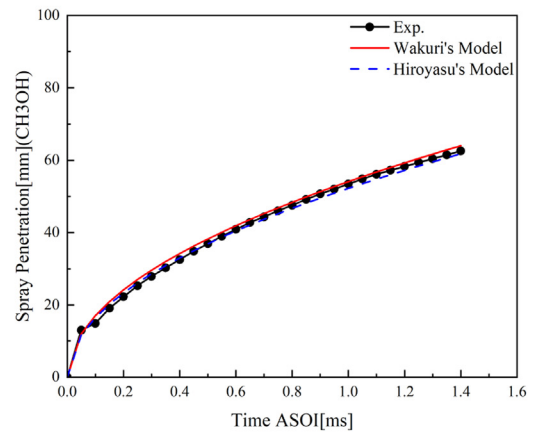
D=0.12mm P=112MPa



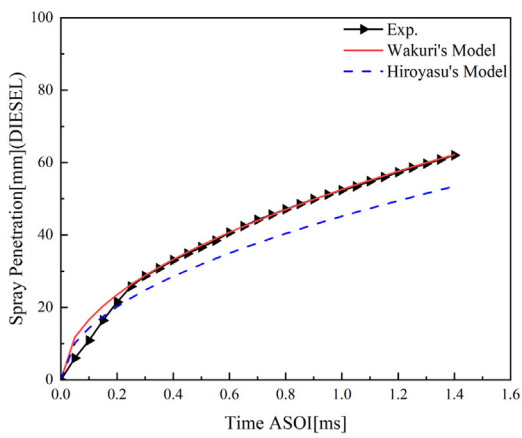
D=0.12mm P=122MPa



D=0.15mm P=100MPa

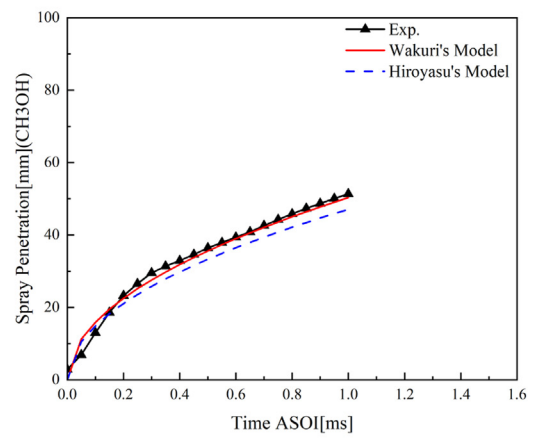


D=0.15mm P=100MPa



D=0.18mm P=40MPa

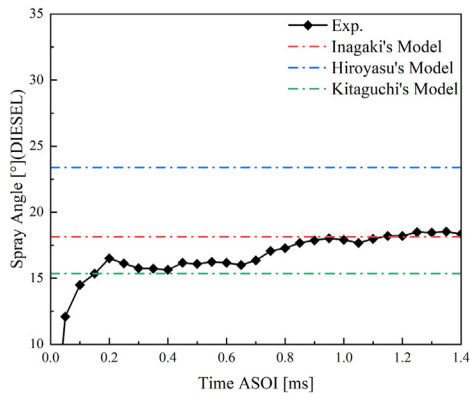
Diesel



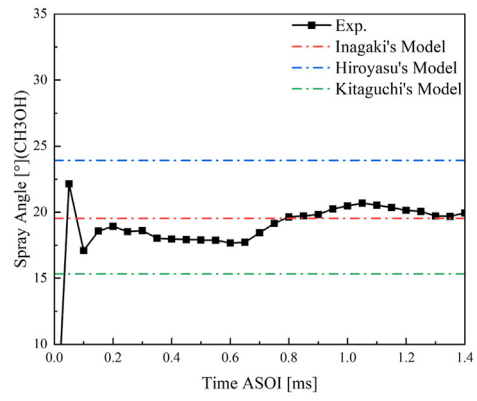
D=0.18mm P=47MPa

Methanol

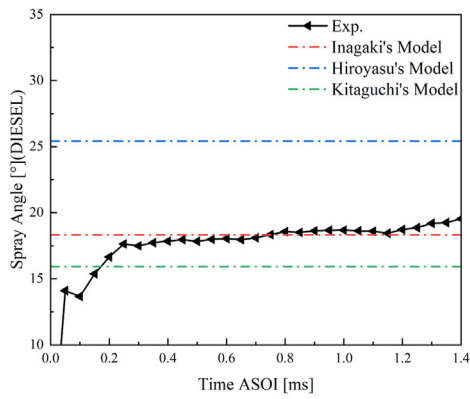
Fig. 7. The experimental values and calculated values of spray tip penetration.



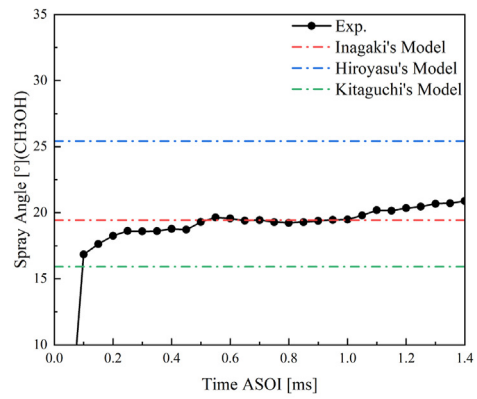
D=0.12mm P=112MPa



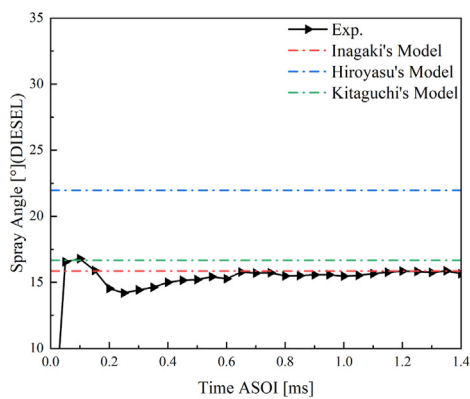
D=0.12mm P=122MPa



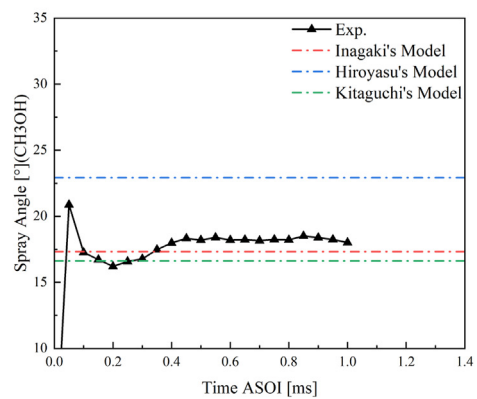
D=0.15mm P=100MPa



D=0.15mm P=100MPa



D=0.18mm P=40MPa

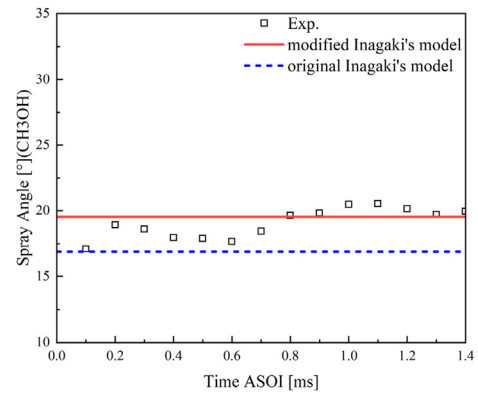
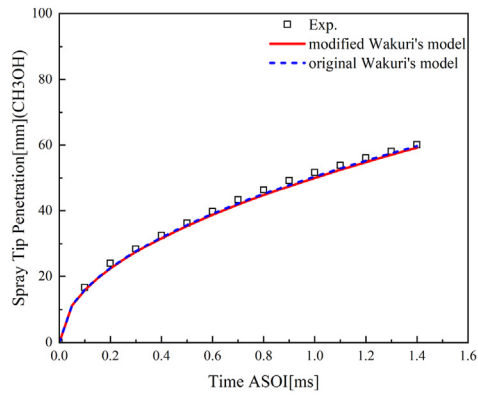


D=0.18mm P=0.47MPa

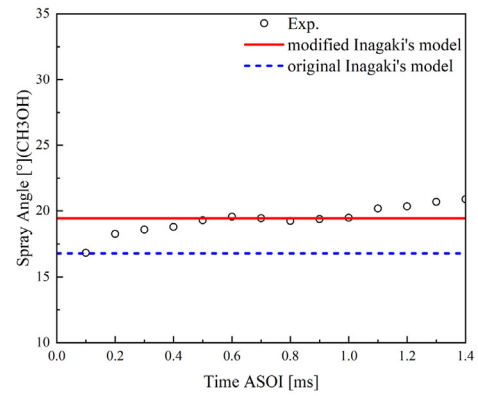
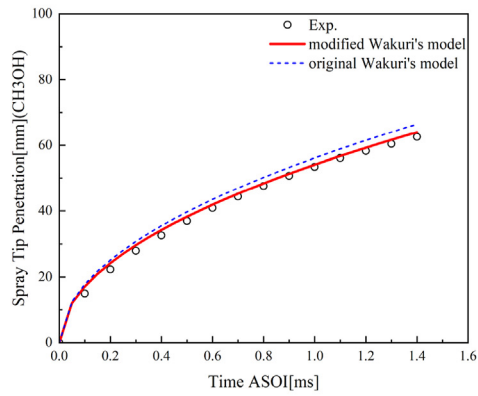
Diesel

Methanol

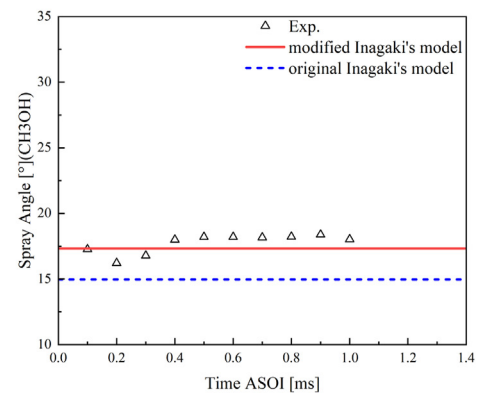
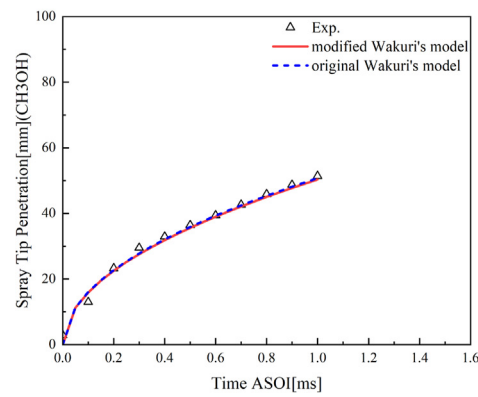
Fig. 8. The experimental values and calculated values of spray angle.



D=0.12mm P=122MPa



D=0.15mm P=100MPa



D=0.18mm P=47MPa

Fig. 9. Optimization of methanol spray tip penetration and spray angle.

According to the above analysis, it is possible to deduce that the empirical model of diesel spray tip penetration and spray angle can predict the methanol spray angle quite well. Among them, Wakuri's model and Inagaki's model with the modified constants show the highest accuracy separately in spray tip penetration and spray angle.

4.2. Optimization of empirical models

Fig. 9 shows the optimization of the empirical models of methanol spray tip penetration and spray angle. To evaluate the applicability of similarity theory, this section mainly explains the optimization of Wakuri's model and Inagaki's model. Wakuri's model predicts with high accuracy that the error is within 3 mm, regardless of using diesel or methanol constants. On the other hand, Inagaki's model differs significantly before and after optimization. The empirical model of diesel significantly underestimates the spray angle of methanol, with an error of approximately 2.5° from the modified model under different conditions. The modified spray tip penetration and spray angle models are as follows:

$$S = 1.264 \left(\frac{\Delta P}{\rho_a} \right)^{0.25} \left(\tan \frac{\theta}{2} \right)^{-0.5} (d)^{0.5} t^{0.5} \tag{26}$$

$$\theta_s = 0.00176 \left(\frac{\rho_a}{\mu_a^2} \right)^{0.25} \Delta P^{0.18} \left(\frac{l}{d} \right)^{-0.14} \tag{27}$$

The spray shapes were simplified as regular geometric shapes so that we could use the models to calculate spray area and spray volume. Based on this hypothesis, linear regression analysis was used to determine the relationship between the experimental and calculated values of the spray area. Fig. 10 shows the results of linear regression analysis obtained from experimental data, demonstrating a high linear correlation between the experimental and calculated values. With a new constant C = 0.94 based on equation (8), Fig. 11 illustrates the variation of the experimental and calculated values of the methanol spray area over time. The methanol spray area shows a linear relationship with time, and the revised empirical model can exactly predict the methanol spray area:

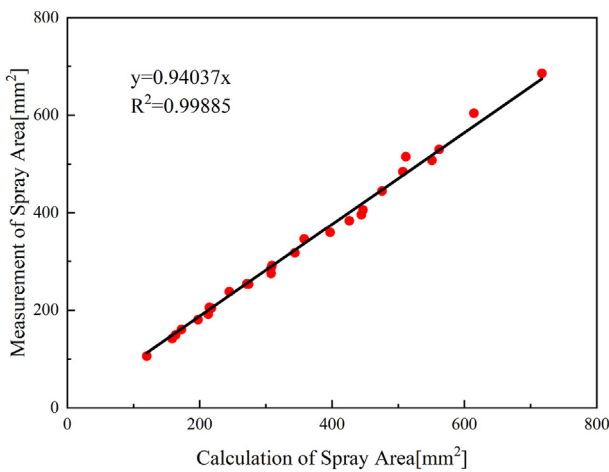


Fig. 10. Comparison of spray area between measurements and calculation.

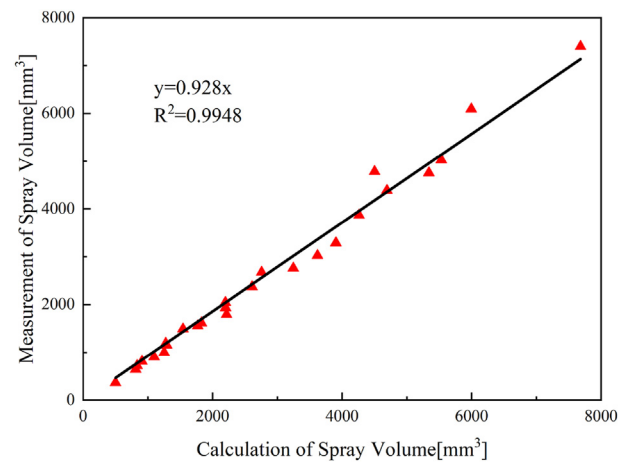


Fig. 12. Comparison of spray volume between measurements and calculation.

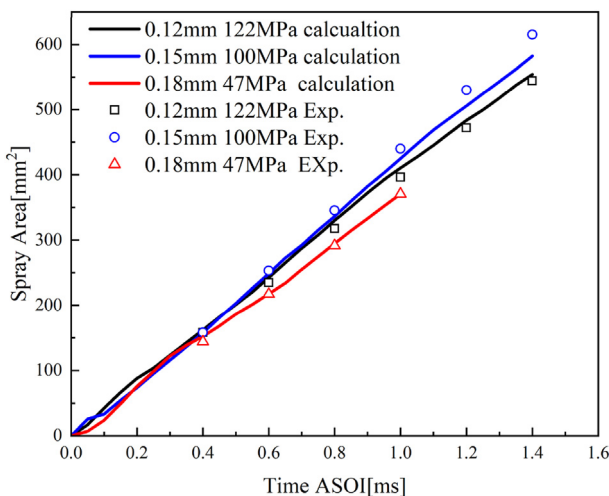


Fig. 11. Measurement values and modified calculated values of the methanol spray area.

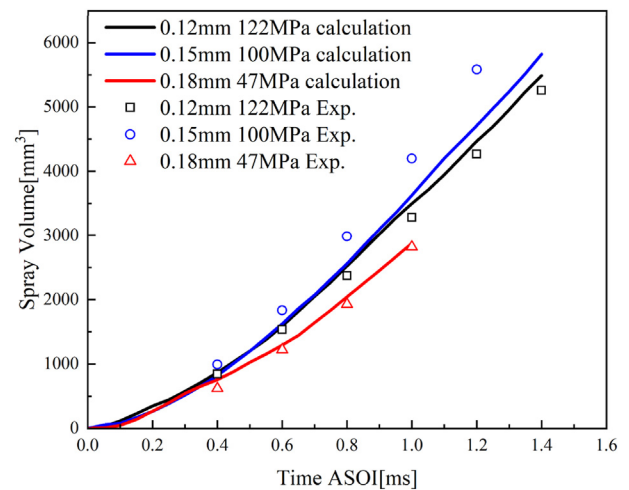


Fig. 13. Measurement values and modified calculation values of methanol spray volume.

$$A = 0.94 \frac{S^2 \tan \frac{\theta}{2} \left(1 + 0.5\pi \tan \frac{\theta}{2}\right)}{\left(1 + \tan \frac{\theta}{2}\right)^2} \quad (28)$$

Fig. 12 shows the relationship between the experimental and calculated values of the spray volume of methanol sprays by linear regression analysis. The experimental values are linearly correlated with the calculated values. The constant $C = 0.93$ is based on equation (9). Fig. 13 illustrates the variation of the experimental and calculated values of the methanol spray volume over time. In the case of 0.15 mm-100 MPa and 0.18 mm-47 MPa, the accuracy of the model is high, while there is an obvious error for 0.12 mm-122 MPa. There are several reasons for the phenomenon: the spray grows fastest under 0.12 mm-122 MPa condition, at the same time it also has the largest spray tip penetration and the largest contact area between the spray and the ambient gas, leading to the highest fuel-air mixing degree. More spray boundary folding appears, and the spray shape becomes more irregular and deviates further from the assumption. As a result, the prediction accuracy is reduced. The following is the model of methanol spray volume:

$$V = \frac{1}{3} \pi S^3 \frac{0.93 \left(\tan \frac{\theta}{2}\right)^2 \left(1 + \tan \frac{\theta}{2}\right)}{\left(1 + \tan \frac{\theta}{2}\right)^3} \quad (29)$$

4.3. Similarity theory

4.3.1. Spray profiles

Fig. 14 describes the spray profiles of diesel and methanol under similarity conditions. Under similarity conditions, methanol, and diesel exhibit a similar trend in development. At the same moment after the start of injection, the injector with a smaller nozzle diameter exhibits smaller spray tip penetration and spray angle, and the overall spray pattern appears to be slender. With the increasing nozzle diameter and injection pressure, the spray development accelerates, leading to the rising instability of the spray and the irregular shape of the spray head.

Additionally, it can be seen from the grayscale of the images that in the late stage of injection, as the nozzle diameter and the injection pressure increase, the droplets become denser, especially at the spray

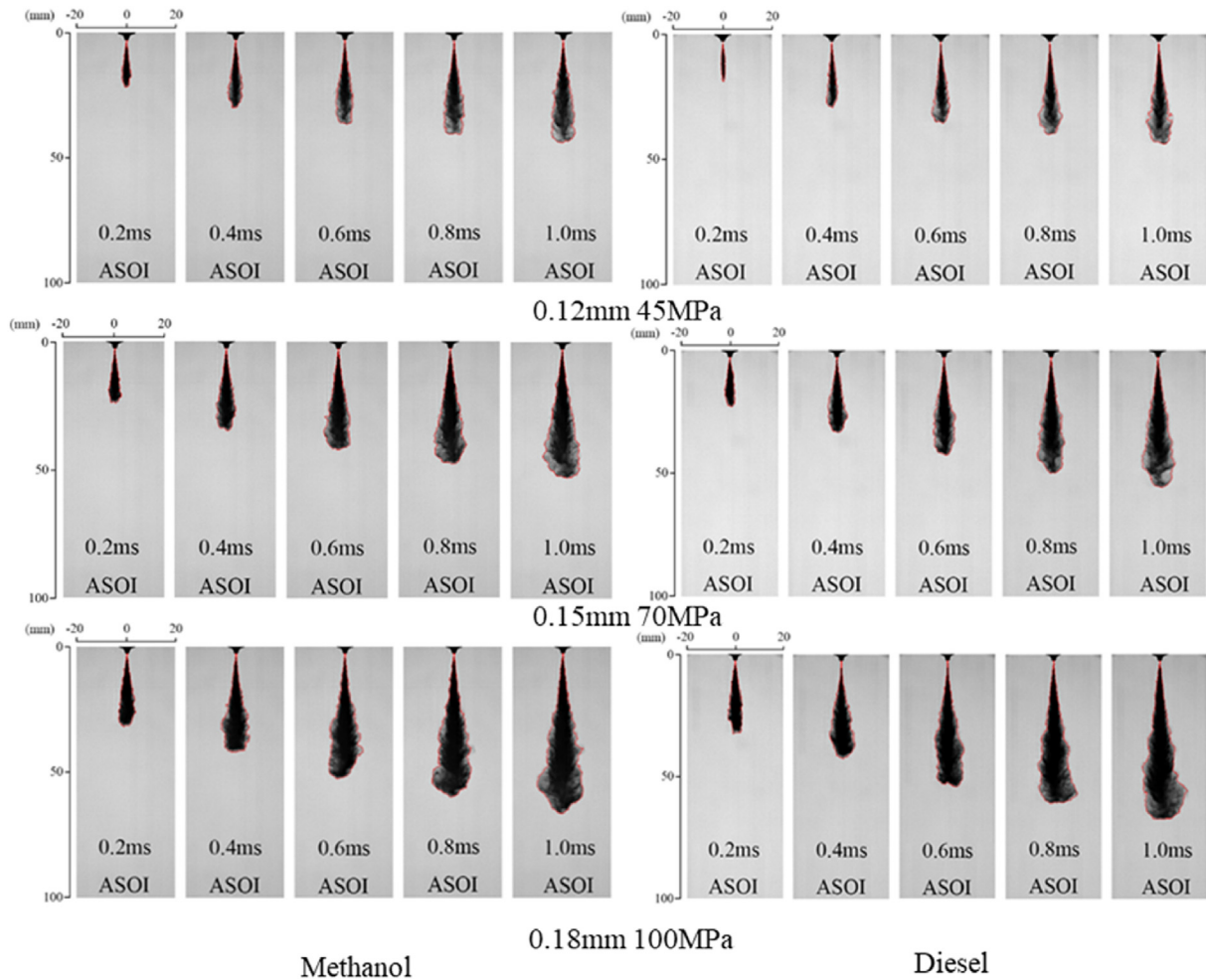
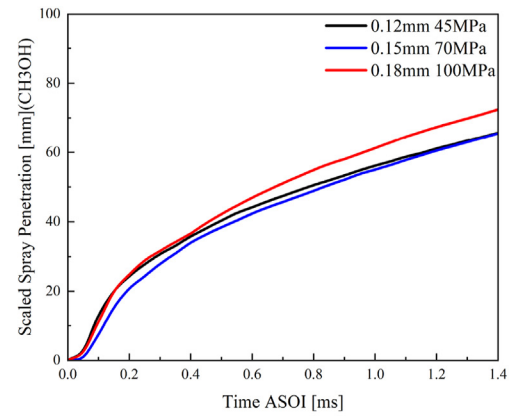
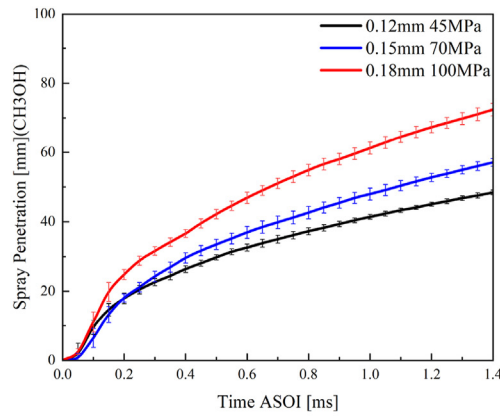


Fig. 14. Spray profiles under similarity condition.

Methanol



Diesel

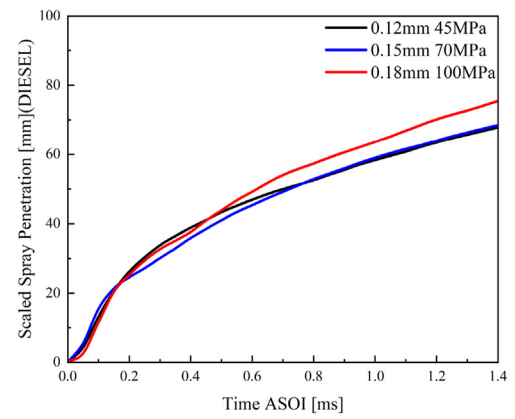
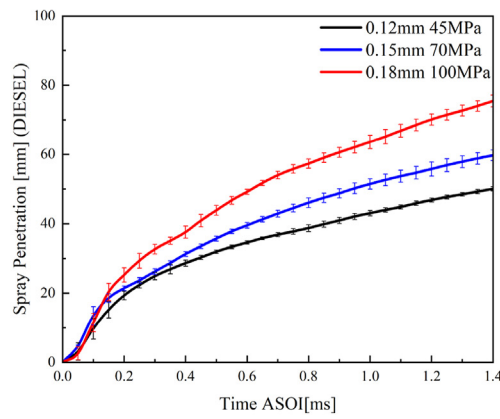


Fig. 15. Original and scaled spray tip penetration of diesel and methanol.

head. At the same ASOI, the injector with a larger nozzle diameter and injection pressure produces more fuel, which has enough kinetic energy at the outlet to force more droplets to move forward.

4.3.2. Spray tip penetration

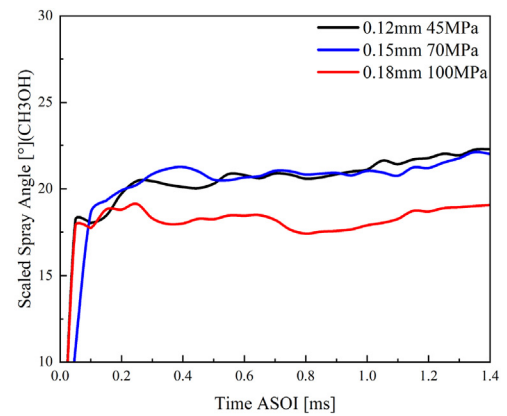
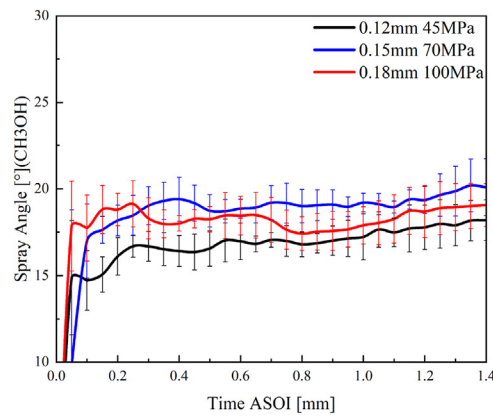
Fig. 15 presents the original and scaled spray tip penetration of diesel and methanol sprays under similarity conditions. The spray characteristic parameters of nozzles with 0.12 mm and 0.15 mm diameters are scaled relative to those of the nozzle with 0.18 mm diameter. The spray tip penetration is scaled by $r^{0.75}$. As shown in Fig. 15, the original spray tip penetration of diesel and methanol sprays follows the same trend: throughout the whole injection process, the spray tip penetration and spray tip velocity of 0.18 mm-100 MPa are the highest all the time, followed by 0.15 mm-70 MPa and then 0.12 mm-45 MPa. The differences in spray tip penetration among the three conditions increase over time. The curves of the scaled spray tip penetration under the three conditions almost overlap when diesel sprays after 0.6ms ASOI and methanol sprays after 0.4ms ASOI can achieve good similarity. After the mentioned moment, 0.12 mm-45 MPa and 0.15 mm-70 MPa conditions continue to maintain a high degree of similarity, but the gap becomes larger between 0.18 mm and 100 MPa and the other two conditions. It shows a decrease

in the practicality of the similarity theory in the late stage of injection. Compared to diesel, methanol has a slightly smaller spray tip penetration, but the development trends are roughly the same. Therefore, the similarity theory of diesel spray characteristics is still applicable to methanol.

4.3.3. Spray angle

Fig. 16 shows the original and scaled spray angle of diesel and methanol sprays under similarity conditions. The spray angle is scaled by $r^{0.5}$. Unlike the spray tip penetration, the original spray angle was the largest under 0.15 mm-70 MPa, followed by 0.18 mm and 0.12 mm, and the difference among the three conditions is not significant. The spray angle is mainly affected by ambient density, viscosity, nozzle structure, and injection pressure. Under similarity conditions, the ambient density and viscosity are the same. According to equation (5), the changes in nozzle diameter and injection pressure under the three experimental conditions have a negligible effect on the spray angle, so the sprays don't strictly follow the similarity theory that the larger nozzle diameter results in the larger spray angle. The empirical model of spray tip penetration has limitations, which are only suitable for predicting the steady spray angle, not for dynamic analysis. Although the scaled spray angles of 0.12 mm-45 MPa and 0.15 mm-70MPa are closer, due to the little

Methanol



Diesel

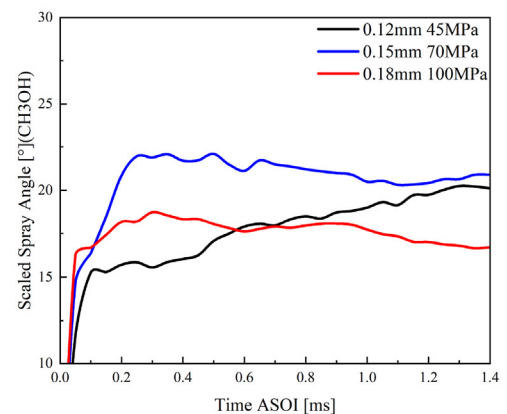
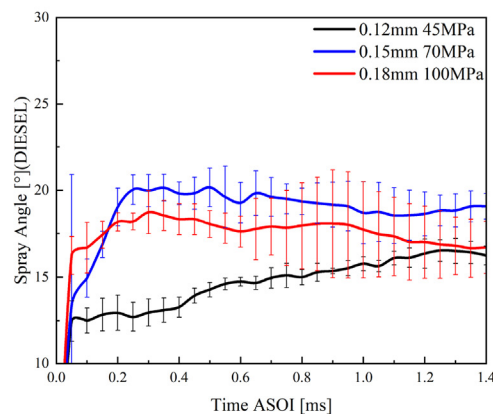


Fig. 16. Original and scaled spray angle of diesel and methanol.

difference in the original spray angle of the three, they are much higher than that of 0.18 mm-100 MPa. The spray angle of methanol is larger than that of diesel, and the spray angle of methanol is more stable during the whole injection process, so the results after scaling are better than that of diesel, except for 0.18 mm-100 MPa condition.

5. Conclusion

Based on optical experiments of high-pressure methanol and diesel sprays, this study applied and modified empirical models to predict the spray characteristics of high-pressure methanol sprays under non-evaporating conditions. Combined with the diesel similarity theory, an evaluation of methanol spray was conducted under similarity conditions. The main conclusions are presented below:

1. The empirical models of diesel spray tip penetration can predict methanol sprays, with the Wakuri model providing the best predictions. In terms of spray angle, Inagaki's model is the most accurate, while the other models deviate significantly from the experimental values. It is feasible to study high-pressure methanol sprays with empirical models of diesel sprays.
2. The empirical models of diesel were modified respectively. After correction, accurate predictions of methanol spray characteristics can be achieved.
3. Under similarity conditions, the application of diesel similarity theory to methanol spray shows a high level of matching degree on spray tip penetration, but not as effective in spray angle after scaling. The best application of the similarity theory is observed under 0.12 mm-45 MPa and 0.15 mm-70 MPa. The accuracy of the diesel similarity

theory reduces greatly when the nozzle diameter and the injection pressure greatly change in comparison with the original injector.

CRediT authorship contribution statement

Pengbo Dong: Writing – review & editing, Conceptualization. **Yifan Zhang:** Writing – original draft, Formal analysis. **Yang Wang:** Methodology, Data curation. **Wuqiang Long:** Supervision. **Jiangping Tian:** Resources. **Hua Tian:** Visualization. **Keiya Nishida:** Supervision.

Declaration of competing interest

We declare that we have no known competing financial interests or personal relationships that could have appeared to influence the work reported in this paper.

Acknowledgement

This work was financially supported by the National Key R&D Program of China (No. 2022YFB4300700).

References

- Brijesh, P., Sreedhara, S., 2013. Exhaust emissions and its control methods in compression ignition engines: a review. *Int. J. Automot. Technol.* 14 (2), 195–206. <https://doi.org/10.1007/s12239-013-0022-2>.
- Chikahisa, T., Murayama, T., 1990. Theory on combustion similarity for different-sized diesel engines. *JSME International Journal, Series 2: Fluids Engineering, Heat Transfer, Power, Combustion, Thermophysical Properties* 33 (2). https://doi.org/10.1299/jsmeb1988.33.2_395.

- Delacourt, E., Desmet, B., Besson, B., 2005. Characterisation of very high pressure diesel sprays using digital imaging techniques. *Fuel* 84 (7–8), 859–867. <https://doi.org/10.1016/j.fuel.2004.12.003>.
- Do, T.N., Kim, J., 2019. Process development and techno-economic evaluation of methanol production by direct CO₂ hydrogenation using solar-thermal energy. *J. CO₂ Util.* 33, 461–472. <https://doi.org/10.1016/j.jcou.2019.07.003>.
- Farzaneh, F., Jung, S., 2023. Lifecycle carbon footprint comparison between internal combustion engine versus electric transit vehicle: a case study in the U.S. *J. Clean. Prod.* 390 (March 1). <https://doi.org/10.1016/j.jclepro.2023.136111>.
- Fayyazbakhsh, A., Bell, M.L., Zhu, X., Mei, X., Koutný, M., Hajinajaf, N., 2022. Engine emissions with air pollutants and greenhouse gases and their control technologies. *J. Clean Prod* 376, 134260. <https://doi.org/10.1016/j.jclepro.2022.134260>.
- Ghosh, A., Ravikrishna, R.V., 2021. Evaporating spray characteristics of methanol-in-diesel emulsions. *Fuel* 290. <https://doi.org/10.1016/j.fuel.2020.119730>.
- Gong, Y., Liu, S., Li, Y., 2007. Investigation on methanol spray characteristics. *Energy Fuel* 21 (5), 2991–2997. <https://doi.org/10.1021/ef0605089>.
- Hiroyasu, H., Arai, M., 1990. Structures of fuel sprays in diesel engines. *SAE Technical Paper* 900475. <https://doi.org/10.4271/900475>.
- Kitaguchi, K., Hatori, S., Hori, T., Senda, J., 2012. Optimization of breakup model using LES of diesel spray. *Atomization Sprays* 22 (1). <https://doi.org/10.1615/AtomizSpr.2012004610>.
- Levich, V.G., Tobias, C.W., 1963. Physicochemical hydrodynamics. *J. Electrochem. Soc.* 110 (11), 251C. <https://doi.org/10.1149/1.2425619>. DOI: 10.1149/1.2425619.
- Lloyd, A.C., Cackette, T.A., 2001. Diesel engines: environmental impact and control. *J. Air Waste Manag. Assoc.* 51 (6), 809–847. <https://doi.org/10.1080/10473289.2001.10464315>.
- Monnerie, N., Gan, P.G., Roeb, M., Sattler, C., 2020. Methanol production using hydrogen from concentrated solar energy. *Int. J. Hydrogen Energy* 45 (49), 26117–25. <https://doi.org/10.1016/j.ijhydene.2019.12.200>.
- Matamis, A., Lonn, S., Tuner, M., Andersson, O., Richter, M., 2020. Optical characterization of methanol sprays and mixture formation in a compression-ignition heavy-duty engine. *SAE Technical Paper*. <https://doi.org/10.4271/2020-01-2109>.
- Inagaki, K., Mizuta, J., Kawamura, K., Idota, Y., Hashizume, T., 2016. Theoretical study on spray design for small-bore diesel engine. *SAE Technical Paper*, 2016-01-0740. <https://doi.org/10.4271/2016-01-0740>.
- Naber, J.D., Siebers, D.L., 1996. Effects of gas density and vaporization on penetration and dispersion of diesel sprays. *SAE Technical Paper* 960034. <https://doi.org/10.4271/960034>.
- Ni, P., Wang, X., Li, H., 2020. A review on regulations, current status, effects and reduction strategies of emissions for marine diesel engines. *Fuel* 279, 118477. <https://doi.org/10.1016/j.fuel.2020.118477>.
- Ravi, S.S., Osipov, S., Turner, J.W.G., 2023. Impact of modern vehicular technologies and emission regulations on improving global air quality. *Atmosphere* 14 (7). <https://doi.org/10.3390/atmos14071164>.
- Shi, Y., Reitz, R.D., 2008. Study of Diesel Engine Size-Scaling Relationships Based on Turbulence and Chemistry Scales. *SAE Technical Paper* 2008-01-0955.
- Song, J., Li, M., Wang, S., Ye, T., 2022. To what extent does environmental regulation influence emission reduction? Evidence from local and neighboring locations in China. *Sustainability* 14 (15). <https://doi.org/10.3390/su14159714> from. <http://www.mdpi.com/2071-1050/14/15/9714>.
- Su, S., Ge, Y., Wang, X., Zhang, M., Hao, L., Tan, J., Shi, F., Guo, D., Yang, Z., 2020. Evaluating the in-service emissions of high-mileage dedicated methanol-fueled passenger cars: regulated and unregulated emissions. *Energies* 13 (11). <https://doi.org/10.3390/en13112680> from. <https://www.mdpi.com/1996-1073/13/11/2680>.
- Wakuri, Y., Fujii, M., Amitani, T., Tsuneya, R., 1959. Studies on the penetration of fuel spray of diesel engine. *Transactions of the Japan Society of Mechanical Engineers* 25 (156), 820–826. <https://doi.org/10.1299/kikai1938.25.820>.
- Wang, Y., Dong, P., Long, W., Tian, J., Wei, F., Wang, Q., Cui, Z., Li, B., 2022. Characteristics of evaporating spray for direct injection methanol engine: comparison between methanol and diesel spray. *Processes* 10 (6). <https://doi.org/10.3390/pr10061132>.
- Wu, Y., Wang, C., Huang, C., Wang, W., Jin, C., Zhang, Z., Zhang, X., Zheng, Z., Liu, H., Yao, M., 2024. The combustion and emission characteristics of pure methanol as a substitute fuel for compression ignition engines. *Int. J. Green Energy* 21 (14), 3313–3329. <https://doi.org/10.1080/15435075.2024.2376714>.
- Yang, L., Yu, B., Yang, B., Chen, H., Malima, G., Wei, Y.M., 2021. Life cycle environmental assessment of electric and internal combustion engine vehicles in China. *J. Clean. Prod.* 285. <https://doi.org/10.1016/j.jclepro.2020.124899>.
- Zhang, Z., Ding, X., Yang, X., Tu, W., Wang, L., Zou, S., 2021. Shedding light on CO₂: catalytic synthesis of solar methanol. *EcoMat* 3 (1). <https://doi.org/10.1002/eom2.12078>.
- Zhou, X., Li, T., Lai, Z., Huang, S., 2021a. Similarity of split-injected fuel sprays for different size diesel engines. *Int. J. Engine Res.* 22 (3), 1028–1044. <https://doi.org/10.1177/1468087419849771>.
- Zhou, X., Li, T., Lai, Z., Wang, B., 2018. Scaling fuel sprays for different size diesel engines. *Fuel* 225, 358–369. <https://doi.org/10.1016/j.fuel.2018.03.167>.
- Zhou, X., Li, T., Wei, Y., Wang, N., 2020. Scaling liquid penetration in evaporating sprays for different size diesel engines. *Int. J. Engine Res.* 21 (9), 1662–1677. <https://doi.org/10.1177/1468087419889835>.
- Zhou, X., Li, T., Yi, P., 2021b. The similarity ratio effects in design of scaled model experiments for marine diesel engines. *Energy* 231. <https://doi.org/10.1016/j.energy.2021.121116>.
- Pucilowski, M., Jangi, M., Shamun, S., Tuner, M., Bai, X.S., 2017. The effect of injection pressure on the NO_x emission rates in a heavy-duty DICI engine running on methanol. *SAE Technical Papers* 2017-01-2194 2017. <https://doi.org/10.4271/2017-01-2194>.
- Svensson, M., Tuner, M., Verhelst, S., 2022. Low load ignitability of methanol in a heavy-duty compression ignition engine. *SAE Technical Paper*. <https://doi.org/10.4271/2022-01-1093>, 2022-01-1093.
- García, A., Monsalve-Serrano, J., Guzmán Mendoza, M., Gaillard, P., Durrett, R., Vassallo, A., Pesce, F., 2023. Evaluation of neat methanol as fuel for a light-duty compression ignition engine. *SAE Technical Papers* 2023-24-0047. <https://doi.org/10.4271/2023-24-0047>.
- Luo, H., Liu, L., Nishida, K., Zhou, W., 2024. Development and utilization on green energy in marine powertrain: challenges and opportunities. *Green Energy and Resources* 2. <https://doi.org/10.1016/j.gerr.2024.100076>.